JOURNAL OF AIRCRAFT
Vol. 47, No. 3, May–June 2010

# Optimal Design of Tow-Placed Fuselage Panels for Maximum Strength with Buckling Considerations

Ahmad Alhajahmad,* Mostafa M. Abdalla,† and Zafer Gürdal‡
*Delft University of Technology, 2629 HS Delft, The Netherlands*

DOI: 10.2514/1.40357

**The introduction of advanced tow-placement machines has made it possible to fabricate novel variable-stiffness composite structures where the fiber orientation angle varies continuously within each ply and throughout the structure. This manufacturing capability allows designers of composites to use the fiber orientation angle as design variable in their analysis, not only for each ply as with conventional composites, but at each point within a ply. Consequently, beyond the improvements that can be accomplished with traditional composites with straight fibers, the directional material properties of composites can be fully exploited to improve the laminate performance. In this paper, design tailoring for the pressure pillowing problem of a fuselage panel bounded by two frames and two stringers is addressed using tow-placed steered fibers. The panel is modeled as a two-dimensional plate loaded by out-of-plane pressure and in-plane loads. A Python-ABAQUS script is developed to perform the linear and geometrically nonlinear finite element analyses of variable-stiffness panels. The design objective is to determine the optimal fiber paths within each ply of the laminate for maximum load carrying capacity and for maximum buckling capacity. Simulated-annealing algorithm is used to solve the optimization problems. Optimal designs are obtained for different loading cases and boundary conditions. As a basis of comparison, a practical constant-stiffness quasi-isotropic design is used. Numerical results indicate that by placing the fibers in their optimal spatial orientations within each ply, the load carrying capacity and the buckling load of the structure can be substantially improved compared with traditional straight fiber designs. It is shown that laminates optimized for maximum failure load have buckling loads that are higher than those for quasi-isotropic laminates. On the other hand, laminates optimized for maximum buckling load fail at load levels lower than laminates optimized for maximum failure load. However, the failure loads of those laminates may still be higher than those for their quasi-isotropic counterparts.**

## Nomenclature

| | | |
|---|---|---|
| $a$, $b$ | = | length and width of the panel |
| $F$ | = | failure index |
| $F_x$ | = | axial tensile load |
| $F_y$ | = | hoop tensile load |
| $F_x^B$ | = | axial compressive load |
| $N$ | = | total number of plies |
| $N_x$ | = | stress resultant in $x$ direction |
| $N_y$ | = | stress resultant in $y$ direction |
| $N_{xy}$ | = | shear stress resultant |
| $P$ | = | pressure load |
| $R_f$ | = | radius of fuselage |
| $T_0$ | = | fiber orientation angle at the panel center |
| $T_1$ | = | fiber orientation angle at the panel ends |
| $t$ | = | ply thickness |
| $\lambda^f$ | = | failure load |
| $\lambda^{cr}$ | = | buckling load |
| $\sigma_1$, $\sigma_2$, $\sigma_{12}$ | = | stresses in the principal material directions |

## I. Introduction

ONE of the primary advantages of using fiber-reinforced laminated composites in structural design is the ability to change the stiffness and strength of the laminate by designing the laminate stacking sequence in order to improve its performance. This flexibility to design the stacking sequence of the laminate is typically referred to as laminate tailoring. Tailoring is traditionally achieved by keeping the fiber orientation angle within each layer constant throughout a component resulting in constant-stiffness structure. By limiting each layer to a single orientation over the entire component, the designer is unable to fully exploit the directional material properties offered by advanced composites. A simple method for improved tailoring is the introduction of discrete jumps in the laminate construction by adding patches of additional layers with different fiber orientations into the component. For example, Biggers and Srinivasan [1] and Biggers and Pageau [2] achieved tailoring by redistributing the layers with specified orientations across the planform of rectangular plates to create beneficial stiffening patterns against compression and shear buckling. Another method of creating variable-stiffness composite structure is by changing the fiber orientation angle continuously within the lamina. Allowing the fibers to curve within the lamina constitutes an advanced tailoring option to account for nonuniform stress states in a continuous manner. By varying the stiffness properties of composite laminates from one point to another, the design space is expanded as compared with the classical stacking sequence design problem. As a consequence, higher performance and/or lighter structures can be obtained.

Hyer and Charette [3] were among the first to investigate the influence of fiber orientation angle around a cutout for a flat plate with a circular hole subjected to axial tensile loads. They chose the fiber orientations so that the fibers in a particular layer were aligned with the principal stress directions in that layer. Their finite element solution demonstrated significant improvement in the load carrying capacity of the curvilinear fiber design compared to a conventional quasi-isotropic design. In an attempt to have a manufacturable representation of fiber orientation angles, Nagendra et al. [4] performed research to develop a method of optimizing tow paths. The tow paths were defined by passing a single curve through a set of control points based on a single cubic non-uniform rational B-splines (NURBS). Using finite elements, they studied optimal frequency and buckling load design of laminated composite plates with a central

Received 11 August 2008; revision received 26 March 2009; accepted for publication 31 March 2009. 

*Ph.D. Student, Faculty of Aerospace Engineering, Aerospace Structures Group, Kluyverweg 1. Member AIAA.

†Assistant Professor, Aerospace Structures Group, Kluyverweg 1. Member AIAA.

‡Professor, Aerospace Structures Chair, Kluyverweg 1. Associate Fellow AIAA.

hole subject to deformations, ply failure, and interlaminar stress constraints, and demonstrated increased performance. In an effort to integrate realistic fabrication techniques into the design of laminates with curvilinear fiber layers research carried out by Gürdal and Olmedo [5,6] introduced a fiber path definition and formulated closed-form and numerical solutions for simple rectangular plates. The proposed fiber orientation variation was generated from a base curve that changes its orientation angle linearly from one end of the panel to the other, while taking into account constraints on the radius of curvature of the fiber paths. Buckling response of the panels was investigated by varying the fiber orientation in the direction of the applied loads and in a direction perpendicular to the loadings. Improvements in the buckling load of up to 80% over straight fiber configurations were found. In a follow-up design study by Waldhart et al. [7], a parametric study of a small set of variables used in the fiber path definitions indicated increased buckling performance due to the stiffness variation, which in turn caused favorable redistribution of the internal stresses. Minimum weight design of composite structures with curved fibers subject to stress constraints was studied by Parnas et al. [8]. In their study they constructed a bicubic Bezier surface for layer thickness representation and cubic Bezier curves for fiber orientation angles and used coordinates of the control points as design variables.

A challenging problem in aircraft structures associated with thin-walled stiffened structures is the so-called pressure pillowing. Pressurized fuselages and fuel tanks are typical examples of structures in which pressure pillowing is observed. In the case of fuselages, the cabin pressure causes a significant pressure differential through the thickness of the skin. An unstiffened fuselage would carry this internal pressure load as a shell in membrane response, like pressure vessels. However, internal longitudinal and transverse stiffeners (stringers and frames as shown in Fig. 1) are necessary to carry maneuver loads. The presence of these stiffeners prevents the fuselage skin from expanding as a membrane, and the skin bulges, or pillows, within each panel bay under the action of the internal pressure (see Fig. 2). When the skin is restrained against out-of-plane expansion at the stiffener locations, a bending boundary layer is formed causing bending stress concentrations. Such stresses can cause peeling of the skin-stiffener interface, and hence designs have to be usually modified to account for them.

An experimental and analytical study of the nonlinear response and failure characteristics of internally pressurized constant-stiffness composite fuselage panels with clamped edges was performed by Boitnott et al. [9]. The study showed that the graphite-epoxy specimens failed at their edges where the magnitudes of local bending gradients and interlaminar stresses are maximum. Recently, design tailoring for pressure pillowing using a variable-stiffness concept based on steered fibers has been investigated by Alhajahmad et al. [10]. The pressure pillowing problem was modeled as a one-dimensional clamped–clamped beam plate subjected to pressure and in-plane compressive loads. Optimal fiber paths along the beam-plate length for minimum weight subject to strength constraints were determined. It was shown that by using steered fibers the pressure pillowing problem can be alleviated, and lighter laminates can be designed compared with designs with straight fibers. In a follow-up study [11], the problem was modeled as a two-dimensional plate subjected to pressure and in-plane loads, and the objective was to determine the optimal fiber paths over the panel for maximum failure loads. This latter study demonstrated that by designing one ply in the laminate lay-up using steered fibers, the pressure pillowing problem can be alleviated and the load carrying capacity of the panels can be improved compared with traditional angle-ply laminates with straight fibers.

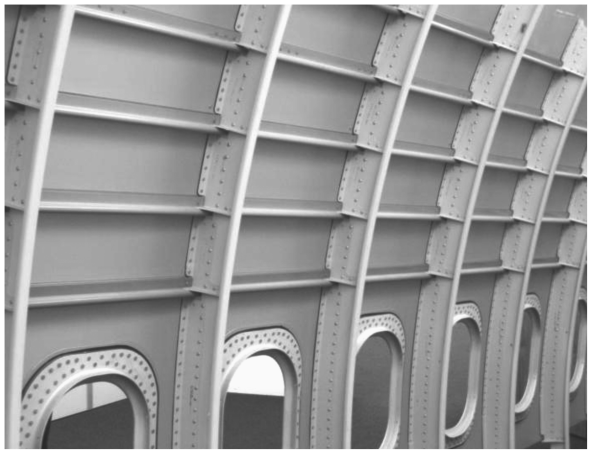

**Fig. 1 Stiffened structure of a pressurized fuselage (courtesy of Fiber Metal Laminates Center of Competence, Delft University of Technology).**

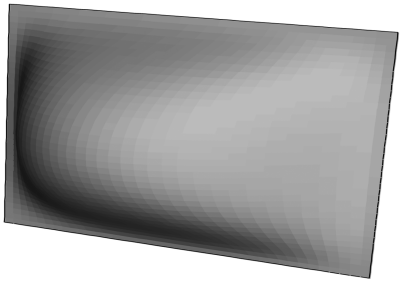

**Fig. 2 Pillowed panel.**

In the current paper, design tailoring for the pressure pillowing problem of a fuselage panel is addressed using steered fibers in multilayered composite laminates. The design objective is to determine the optimal fiber paths within each ply of the laminate for maximum strength and maximum buckling performance. Variable-stiffness designs obtained will be compared with their constant-stiffness counterparts.

In what follows, we will explain the problem and describe the fiber paths that will be adopted for this work. Also, a brief explanation about the finite element model, failure analysis, and optimization formulation will be provided. Finally, we will present optimized results and discussions and draw conclusions.

## II. Problem Description

In this paper, a pressurized fuselage skin bounded by two stringers and two frames is modeled as a two-dimensional plate. It is assumed that the skin is a flat, balanced, and symmetric laminate with a variable-stiffness lay-up. The laminate is loaded in two steps. In the first loading step, a uniform pressure $P$ is applied. It is assumed that the pressure load also includes in-plane loads on the panel due to pressurization of a fuselage of radius $R_f$. The in-plane loads are approximately translated into an axial tensile load $F_x$, and a hoop tensile load $F_y$, calculated as

$$F_x = \frac{PR_f}{2} b \qquad F_y = PR_f a \tag{1}$$

where $a$ and $b$ are the length and the width of the plate, respectively. The pressure and hence the tensile loads are incremented by means of a scaling factor $\lambda_1$ in the first loading step. It should be noted that the relations given by Eq. (1) are valid only for unstiffened cylindrical shells because the skin loads will be reduced according to the stiffness contributions from the stringers and frames. However, for the sake of simplicity, these contributions are neglected in the present study. In the second loading step, an additional axial compressive load $F_x^B$, which may result from fuselage bending, is applied. This latter load is incremented by means of a scaling factor $\lambda_2$ while keeping $\lambda_1$ fixed at the end of the first loading step. The fuselage panel model is shown in Fig. 3.

Two different boundary conditions will be modeled. Since the panel edges are bounded by different structural elements like stringers, frames, and other adjacent panels, and typically external

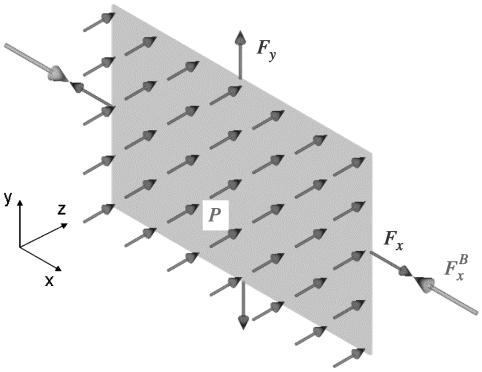


**Fig. 3 Fuselage panel model.**

continuously into the adjacent bays, the boundary conditions of the panel edges can be very complex. In the current work, we assume deformable straight edges. This implies that the out-of-plane displacement of the stringers and frames, due to bending, will be neglected. The boundary conditions of the panel edges will be modeled as the following,

1) Clamped at ($x = 0$, $x = a$) simulating the panel edges at the frame locations and simply supported at ($y = 0$, $y = b$) simulating the panel edges at the stringer locations. This will be denoted by SS-CC.

2) All the panel edges are clamped. This will be denoted by CC-CC.

## III. Fiber Path Definition

Varying the stiffness throughout the structure requires defining the fiber orientation variations. In this paper, the linear variation of fiber orientation angles introduced by Gürdal and Olmedo [5] will be used. The linear variation along one of the axes, say $\tilde{x}$, which is assumed to be centered along the length $a$ of the panel, is given by

$$\theta(\tilde{x}) = \frac{2(T_1 - T_0)}{a}|\tilde{x}| + T_0 \tag{2}$$

where $T_0$ is the fiber orientation angle at the panel center, $\tilde{x} = 0$, and $T_1$ is the fiber orientation angle at the panel ends, $\tilde{x} = \pm a/2$. For the form mentioned above, a representation of a single layer has been suggested to be $\langle T_0|T_1\rangle$ (note that when $T_0 = T_1$ the fiber orientation becomes constant, i.e., $\theta = T_0 = T_1$), and the corresponding fiber path is given by [5]

$$y = \frac{a}{2(T_1 - T_0)}\left\{-\ell_n\left[\cos\left(T_0 + \frac{2(T_1 - T_0)\tilde{x}}{a}\right)\right] + \ell_n[\cos(T_0)]\right\}$$
$$\text{for } 0 \le \tilde{x} < \frac{a}{2}$$
$$y = \frac{a}{2(T_1 - T_0)}\left\{\ell_n\left[\cos\left(T_1 + \frac{2(T_1 - T_0)\tilde{x}}{a}\right)\right] - \ell_n[\cos(T_1)]\right\}$$
$$\text{for } -\frac{a}{2} \le \tilde{x} < 0 \tag{3}$$

For the current work, we generalize Eq. (2) for multiple layers. Taking into account the coordinate system defined in Fig. 3, we write Eq. (2) as:

$$\theta(x) = \begin{cases} \frac{2}{a}(T_0^{(k)} - T_1^{(k)})x + T_1^{(k)} & \text{for } 0 \le x \le \frac{a}{2} \\ \frac{2}{a}(T_1^{(k)} - T_0^{(k)})x + 2T_0^{(k)} - T_1^{(k)} & \text{for } \frac{a}{2} \le x \le a \end{cases} \tag{4}$$

where $k$ is the layer number.

By replacing $x$ by $y$ and $a$ by $b$ in Eq. (4), the fiber angle variation as a function of $y$ coordinate can be defined, $\theta = \theta(y)$.

## IV. Finite Element Model

The strength and buckling responses of the laminates are obtained using ABAQUS [12] finite element models. Using the ABAQUS scripting interface, a Python[§] script is developed to perform the linear and geometrically nonlinear finite element analyses of variable-stiffness panels. To create the models for variable-stiffness panels, first of all the structure is meshed using S4R ABAQUS elements. Then the nodal connectivity of each element is considered to calculate the centroid of the element by using coordinates of the elements' nodes. Afterward, a local fiber orientation at the element centroid is computed using the fiber orientation definition given in Eq. (4). By using the local fiber orientation, which is assumed to be constant within an element, a stacking sequence is constructed and assigned to the corresponding element. Based on the fiber path function definition, each element may have its own stacking sequence, hence generating variable-stiffness composite structure. To compute the stresses, three through-the-thickness integration points are used for each ply. For example, Fig. 4 illustrates the fiber paths for a layer with $\langle 0°|45°\rangle$ linear orientation variation. Corresponding fiber orientation angle of each element of the finite element mesh is shown in Fig. 5, with each short straight line emitted from the element centroid representing the local fiber orientation for that element.

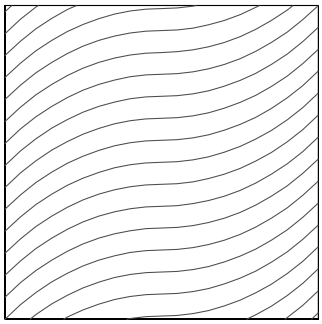

**Fig. 4 Fiber paths for $\langle 0°|45°\rangle$ layer.**

## V. Failure Analysis

The failure load $\lambda^f$ is defined as the load level at which first failure occurs. For the purpose of predicting failure, we use the Tsai–Wu failure criterion. For an orthotropic lamina under plane stress conditions, this criterion is given by

$$F = F_{11}\sigma_1^2 + 2F_{12}\sigma_1\sigma_2 + F_{22}\sigma_2^2 + F_{66}\sigma_{12}^2 + F_1\sigma_1 + F_2\sigma_2 \tag{5}$$

where $F$ is the failure index, $\sigma_1, \sigma_2$, and $\sigma_{12}$ are the in-plane stresses in the principal material directions, and $F_{ij}$ are functions expressed in terms of the strength properties as follows:

$$F_{11} = \frac{1}{X_t X_c}, \qquad F_{22} = \frac{1}{Y_t Y_c}, \qquad F_{66} = \frac{1}{S^2} \qquad F_1 = \frac{1}{X_t} - \frac{1}{X_c}$$
$$F_2 = \frac{1}{Y_t} - \frac{1}{Y_c} \qquad F_{12} = \frac{1}{2X_t^2}[1 - X_t(F_1 + F_2) - X_t^2(F_{11} + F_{22})] \tag{6}$$

According to Tsai–Wu criterion, a composite fails when the following condition is violated

$$F \le 1 \tag{7}$$

To apply the Tsai–Wu criterion to variable-stiffness laminates, it must be kept in mind that the location where stresses are maximum may not be the location of failure. Since the fiber orientation also varies as a function of location a complete search of points satisfying the condition in Eq. (7) must be performed. That is,

$$F_{(x,y)} \le 1 \tag{8}$$

[§]Data available online at www.Python.Org [retrieved March 2010].

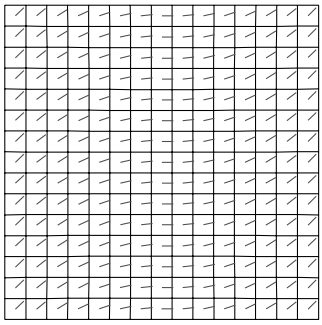

**Fig. 5 Finite element model for ⟨0°|45°⟩ layer.**

## VI. Optimization Formulation

In this paper, the goal of the optimization problems is to determine the optimal fiber paths within each ply of the laminate lay-up for maximum failure load and for maximum buckling load. Mathematically, the problem is formulated as

$$\begin{aligned} &\text{maximize } \lambda(\mathbf{x}) \qquad \text{subject to: } x_i^L \le \mathbf{x} \le x_i^U \\ &i = 1, 2, \ldots \text{number of design variables} \end{aligned} \tag{9}$$

where $\lambda$ is the objective function representing either the failure load, $\lambda^f$, or the buckling load, $\lambda^{cr}$, and $\mathbf{x}$ is a vector of design variables. The design variables that will be used in the current paper are the fiber orientation angles $T_0$ and $T_1$ present in Eq. (4) for each layer. To avoid having excessively large curvatures in the tailored fiber paths, the lower bound and the upper bound constraints on the fiber orientation angles are set to 0 and 90°, respectively. Thus, the optimization problems can be written as

$$\begin{aligned} &\text{maximize } \lambda^f\{T\} \quad \text{or} \quad \lambda^{cr}\{T\} \\ &\text{subject to: } 0^\circ \le T_0^{(k)}, T_1^{(k)} \le 90^\circ \end{aligned} \tag{10}$$

where $k$ is the layer number or the number of pair of adjacent layers in the stacking sequence.

Previous research on variable-stiffness laminates [11] showed that for a given value of $T_0$ the values of the failure load do not increase monotonically when the values of $T_1$ increase. Therefore, searches for an optimal solution using traditional gradient based approaches are likely to be trapped in local optima. Accordingly, the global simulated-annealing (SA) optimizer will be used as the design optimization platform due to its robustness [13].

## VII. Application and Results

Numerical results are generated for square (20 in × 20 in) and symmetric laminates with different variable-stiffness lay-ups. The number of laminate plies is $N = 16$. Each ply has a constant thickness $t = 0.01$ in, i.e., the total thickness is $h = N \cdot t$. The composite material is typical graphite-epoxy with stiffness and strength properties given in Table 1 [14]. The initial pressure load is $P = 15$ psi and the fuselage radius is assumed to be $R_f = 100$ in. The underlying goal of the optimization problems is to determine the optimal fiber paths within each ply of the laminate for maximum failure load and for maximum buckling load. Then, the performance of laminates optimized for maximum failure load will be evaluated for buckling and vice versa (i.e., the strength of laminates optimized for maximum buckling load will be evaluated). Results obtained for variable-stiffness laminates will be compared with those of a practical constant-stiffness quasi-isotropic laminate $[\pm 45^\circ/0^\circ/90^\circ]_{2s}$. (This laminate was used in the literature [3,15] as a datum for comparison between variable-stiffness and constant-stiffness designs.) Also, for some load cases the performance of the optimal variable-stiffness designs will be compared with their optimal straight fiber counterparts.

For maximum strength design, two loading cases are considered for the SS-CC and CC-CC laminates. The first loading case is a laminate subjected to pressure only (no pressure-induced tensile loads), which will be called case I, and the second case is a laminate subjected to a combination of pressure (along with the in-plane tensile loads induced) and compressive loads applied in two steps, as described earlier. In the first loading step, the pressure and the pressure-induced tensile loads are applied. Then the in-plane compressive load is applied in the second loading step, while keeping the loads applied in the first loading step constant. This latter case will be called case II. For case I, the fiber orientation angle within a lamina will be varied as a function of $x$ coordinate only, $\theta = \theta(x)$. For case II, however, the fiber orientation in each layer can either be varied as a function of $x$ coordinate, $\theta = \theta(x)$, or as a function of $y$ coordinate, $\theta = \theta(y)$. Optimal variable-stiffness laminates will be obtained by designing two layers and four layers controlled by independent fiber orientation function in the laminate lay-up. In the first case the laminate has a stacking sequence $[\pm\theta_1/\pm\theta_2]_{2s}$, where $\theta_k = \langle T_0^{(k)}|T_1^{(k)}\rangle$ with $k = 1, 2$. As a result, we will have two different designed plies in the laminate lay-up (a total of 16 plies) with four design variables. The second lay-up is a laminate with a stacking sequence$[\pm\theta_1/\pm\theta_2/\pm\theta_3/\pm\theta_4]_s$. Consequently, we have four different plies in the laminate lay-up with eight design variables to be determined. It should be mentioned that for the latter lay-up, considering the balanced and symmetric conditions, the entire stacking sequence is being designed.

### A. Optimal Designs for Maximum Failure Loads

#### 1. *Case I: Laminate Subjected to Pressure*

In this loading case, the pressure load $\lambda_1 \cdot P$ is increased until laminate first ply failure, $\lambda_1 = \lambda_1^f$. Then the aim is to maximize the pressure failure load by introducing $\lambda_1^f$ as an objective function. Results for variable-stiffness (VS) laminates with two- and four-designed plies are present in Tables 2 and 3, respectively, along with those for constant-stiffness quasi-isotropic designs. It should be recalled that the fiber orientation is a function of $x$ coordinate only, in this loading case.

A glance at Tables 2 and 3 shows that substantial improvements in the load carrying capacity of the laminates can be obtained using steered fibers compared with the quasi-isotropic designs. Moreover, as expected the more tailored plies are involved in the design, the better are the improvements achieved. In an earlier research [11], results for the SS-CC panel revealed that by designing a single layer in the laminate lay-up (i.e., laminates with $[\pm\theta]_{4s}$ lay-up), the variable-stiffness laminates (using the same linear variation of fiber orientation function) produced 11% improvement in the load carrying capacity relative to their straight fiber counterparts. It is obvious that by designing four layers for the same panel, about 70% improvement in the load carrying capacity is achieved with respect to its quasi-isotropic baseline. The layers of the SS-CC laminate are depicted in Fig. 6. It is observed that despite the fact that there is a chance for the fiber paths to converge to straight fibers (i.e., $T_0 = T_1$), all laminates have steered fiber layers only.

#### 2. *Case II: Laminate Subjected to Pressure and In-Plane Loads*

In this case, it is assumed that the pressure and the pressure-induced tensile loads are kept constant ($\lambda_1 = 1, P = 15$ psi) after the

**Table 1 Material properties**

| Material properties | Values |
|---|---|
| $E_1$ | $30 \times 10^6$ psi |
| $E_2$ | $0.75 \times 10^6$ psi |
| $\nu_{12}$ | 0.25 |
| $G_{12}$ | $0.375 \times 10^6$ psi |
| $X_t$ | $150 \times 10^3$ psi |
| $Y_t$ | $6 \times 10^3$ psi |
| $S$ | $10 \times 10^3$ psi |
| $X_c$ | $100 \times 10^3$ psi |
| $Y_c$ | $17 \times 10^3$ psi |

**Table 2 Load carrying capacity improvement (VS vs quasi-isotropic laminates); two-designed layers, $\theta = \theta(x)$**

| Boundary conditions | Laminate | Pressure failure load, $\lambda_1^f$ | Load carrying capacity improvement, % |
|---|---|---|---|
| SS-CC | $[\pm 45/0/90]_{2s}$ | 2.0 | 55.0 |
| —— | $[\pm\langle 88\vert 15\rangle/\pm\langle 10\vert 18\rangle]_{2s}$ | 3.1 | —— |
| CC-CC | $[\pm 45/0/90]_{2s}$ | 2.2 | 22.7 |
| —— | $[\pm\langle 84\vert 24\rangle/\pm\langle 87\vert 68\rangle]_{2s}$ | 2.7 | —— |

**Table 3 Load carrying capacity improvement (VS vs quasi-isotropic laminates); four-designed layers, $\theta = \theta(x)$**

| Boundary conditions | Laminate | Pressure failure load, $\lambda_1^f$ | Load carrying capacity improvement, % |
|---|---|---|---|
| SS-CC | $[\pm 45/0/90]_{2s}$ | 2.0 | 70.0 |
| —— | $[\pm\langle 84\vert 23\rangle/\pm\langle 76\vert 5\rangle/\pm\langle 22\vert 33\rangle/\pm\langle 70\vert 82\rangle]_s$ | 3.4 | —— |
| CC-CC | $[\pm 45/0/90]_{2s}$ | 2.2 | 59.1 |
| —— | $[\pm\langle 36\vert 35\rangle/\pm\langle 60\vert 14\rangle/\pm\langle 90\vert 15\rangle/\pm\langle 90\vert 82\rangle]_s$ | 3.5 | —— |

**Table 4 Comparison between VS and quasi-isotropic laminates; two-designed layers, $\theta = \theta(x)$**

| Boundary conditions | Laminate | Compressive failure load, $\lambda_2^f$ | Load carrying capacity improvement, % | Normalized buckling load | Buckling load improvement, % |
|---|---|---|---|---|---|
| SS-CC | $[\pm 45/0/90]_{2s}$ | 4.02 | 44.8 | 1.0 (14170 lb) | 30.0 |
| —— | $[\pm\langle 0\vert 0\rangle/\pm\langle 90\vert 44\rangle]_{2s}$ | 5.82 | —— | 1.3 | —— |
| CC-CC | $[\pm 45/0/90]_{2s}$ | 3.54 | 50.8 | 1.0 (19982 lb) | 38.0 |
| —— | $[\pm\langle 8\vert 30\rangle/\pm\langle 90\vert 39\rangle]_{2s}$ | 5.34 | —— | 1.38 | —— |

first loading step, and the compressive load $F_x^B = -\lambda_2 \cdot F_x$ is increased until panel failure, $\lambda_2 = \lambda_2^f$. The goal is then to maximize the in-plane compressive failure load by introducing $\lambda_2^f$ as an objective function. Similar to case I, two and four plies are designed in the laminate lay-up for maximum failure loads. In addition, the buckling loads of the laminates optimized for maximum failure loads are computed to assess their buckling resistance compared with baseline quasi-isotropic laminates. For the purpose of comparison, the buckling loads of the quasi-isotropic laminates are $\lambda^{cr} =$ 14170 lb for SS-CC and $\lambda^{cr} =$ 19982 lb for CC-CC laminates. For the results presented in the rest of the paper, the buckling loads of the variable-stiffness designs are normalized by the buckling loads of the corresponding quasi-isotropic laminates as shown in Table 4. The failure loads of the quasi-isotropic laminates and those for the variable-stiffness ones obtained for maximum failure loads using two- and four-designed plies are present in Table 4 and 5, respectively, along with the normalized buckling loads of all laminates. Note that the fiber orientation is a function of the $x$ coordinate for the two-designed plies and a function of either the $x$ coordinate or the $y$ coordinate for the four-designed plies.

It can be seen from Tables 4 and 5 that considerable improvements in the load carrying capacity of the structure can be achieved by using steered fibers compared with the quasi-isotropic straight fiber designs. Also, increasing the number of designed layers improves slightly the load carrying capacity of the variable-stiffness laminates. Varying the fiber orientation along the $y$ direction yields better strength and buckling performance than that along the $x$ direction. It can be observed that the fiber paths of the external layers of the SS-CC laminate have converged to straight fibers with zero or close to zero orientations.

More important, it is apparent that the laminates optimized for maximum failure loads have buckling loads that are also significantly higher than those for quasi-isotropic baselines. The CC-CC panel with $\theta = \theta(y)$, has improvements of 67.2 and 76%, load carrying capacity and buckling capacity, respectively, over its quasi-isotropic counterpart. In an earlier study [11], it was demonstrated that the increase in the load carrying capacity over the constant-stiffness design, obtained for the variable-stiffness design, is mainly due to the stress redistribution throughout the panel, achieved by the steered fibers. To demonstrate the possible reason behind the improved buckling performance resulted from a design intended to improve the panel strength, first we illustrate the layers of the CC-CC panel mentioned above as shown in Fig. 7.

It can be seen from Fig. 7 that all the layers except the external ones have zero fiber orientation near the panel transverse edges ($y = 0$, $y = b$), which results in high local in-plane stiffness. It is intuitive

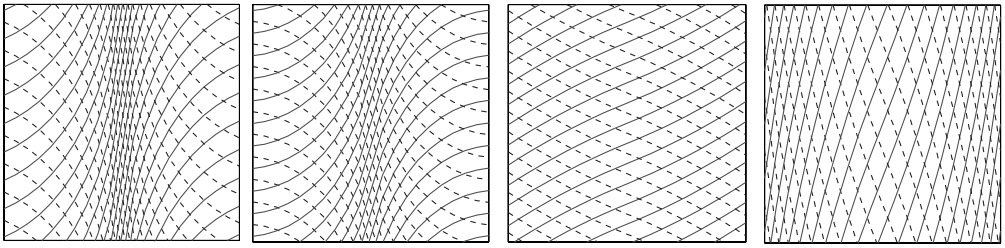


**Fig. 6 Optimal fiber paths for maximum pressure failure load (SS-CC laminate with four-designed layers, $\theta = \theta(x)$).**

**Table 5 Comparison between VS and quasi-isotropic laminates; four-designed layers**

| Boundary conditions | Angle variation | Laminate | Compressive failure load, $\lambda_2^f$ | Load carrying capacity improvement, % | Normalized buckling load | Buckling load improvement, % |
|---|---|---|---|---|---|---|
| SS-CC | - | $[\pm 45/0/90]_{2s}$ | 4.02 | —— | 1.0 | —— |
| —— | $\theta = \theta(x)$ | $[\pm\langle 5\vert 0\rangle/\pm\langle 0\vert 5\rangle/\pm\langle 90\vert 52\rangle/\pm\langle 0\vert 22\rangle]_s$ | 5.94 | 47.8 | 1.41 | 41.0 |
| —— | $\theta = \theta(y)$ | $[\pm\langle 5\vert 0\rangle/\pm\langle 0\vert 10\rangle/\pm\langle 90\vert 0\rangle/\pm\langle 84\vert 86\rangle]_s$ | 6.08 | 51.2 | 1.5 | 50.0 |
| CC-CC | —— | $[\pm 45/0/90]_{2s}$ | 3.54 | —— | 1.0 | —— |
| —— | $\theta = \theta(x)$ | $[\pm\langle 74\vert 64\rangle/\pm\langle 10\vert 0\rangle/\pm\langle 0\vert 8\rangle/\pm\langle 88\vert 54\rangle]_s$ | 5.52 | 55.9 | 1.07 | 7.0 |
| —— | $\theta = \theta(y)$ | $[\pm\langle 15\vert 90\rangle/\pm\langle 24\vert 0\rangle/\pm\langle 50\vert 0\rangle/\pm\langle 60\vert 0\rangle]_s$ | 5.92 | 67.2 | 1.76 | 76.0 |

that the stiffness variation from point to point along the $y$ direction has large influence on the buckling load. To visualize this influence, the distribution of the prebuckling stress resultant in the $x$ direction, $N_x$, across the panel width, is illustrated in Fig. 8.

It is quite clear that the reason for the improved buckling performance is due to the distribution of the applied load across the panel width as a function of the $y$ coordinate. Figure 8 reveals that reasonable portion of the applied load has been transferred toward regions that have high stiffness (near the panel transverse edges), which are supported with respect to the out-of-plane displacements, hence improving the buckling capacity. More details about improving the buckling performance will be discussed in the next section.

An important finding, before moving to the next section, is that the optimization problem for maximum strength, carried out earlier, could have been formulated such that the optimal fiber paths are determined for maximum load carrying capacity with a constraint on the buckling load value not to be less than the buckling load of a quasi-isotropic laminate. However, it is clear now that such a formulation would have resulted in an inactive constraint.

Before moving to the next section, it should be mentioned that the stacking sequence of the quasi-isotropic laminate is not optimal for the strength. For a more fair comparison between the variable-stiffness and constant-stiffness laminates, the optimal stacking sequence of the latter ones should be determined for maximum strength. Therefore, similar to the quasi-isotropic laminates used above the $\pm 45°$ layers will be kept in the lay-up at the top and bottom of the laminate (i.e., the laminate lay-up is $[\pm 45/\theta_1/\theta_2/\theta_3/\theta_4/\theta_5/\theta_6]_s$) and the fiber orientation angles of the rest of layers will be determined. As such, there will be six design variables to be identified. Traditionally, genetic algorithm platforms are used to solve such classical stacking sequence design problems [16] where the design variables are treated as discrete ones and the fiber orientations are restricted to 45, −45, 0, and 90°. To permit more freedom to the design space, however, the design variables are treated as continuous ones and the optimization problem is solved using SA platform. For the SS-CC laminate the optimal stacking sequence is $[\pm 45/89/0/7/0/0/89]_s$ and the corresponding compressive failure load is $\lambda_2^f = 5.24$. For the CC-CC laminate the optimal stacking sequence is $[\pm 45/12/88/90/0/88/0]_s$ and the corresponding failure load is $\lambda_2^f = 4.9$. It is obvious that most of the layers have nearly converged to 0° and 90° orientations for both laminates. A comparison between the variable stiffness where $\theta = \theta(y)$ and the optimal constant-stiffness laminates after casting the laminates mentioned above in the form of the quasi-isotropic ones (i.e., setting the 7 and 12° orientations, in the SS-CC and CC-CC laminates, respectively, to 0° orientations and the 88 and 89 to 90° orientations) is shown in Table 6.

It is evident that by optimizing the stacking sequence of the constant-stiffness laminates, the difference in the load carrying capacity between them and the variable-stiffness ones has dropped significantly compared with the quasi-isotropic laminates, while negligible difference in the buckling load has been observed (note that the buckling loads are normalized with respect to the optimal constant-stiffness laminates).

### B. Optimal Designs for Maximum Buckling Loads

Following the same steps of the design philosophy performed earlier, in this section designs using steered fibers will be obtained for maximum buckling loads. Then, the in-plane compressive failure loads (note that the pressure and the pressure-induced tensile loads are applied in the failure analysis) of these designs are evaluated for comparison. The buckling loads and the failure loads of designed laminates are compared with their quasi-isotropic counterparts. A summary of these results is shown in Tables 7 and 8.

As expected, it is quite obvious from Tables 7 and 8 that substantial improvements in the buckling loads can be achieved using tailored fibers paths compared with the traditional quasi-isotropic baselines.

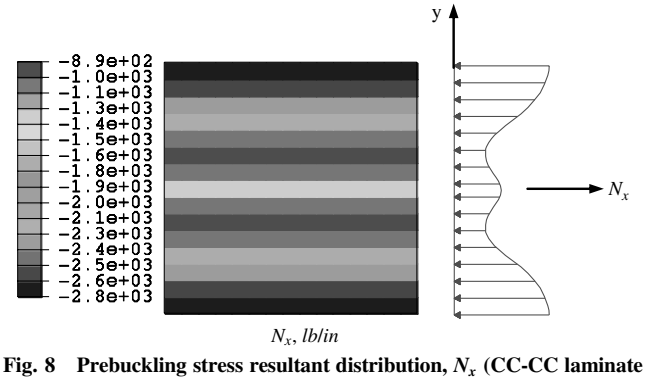


**Fig. 8 Prebuckling stress resultant distribution, $N_x$ (CC-CC laminate with four-designed layers, $\theta = \theta(y)$).**

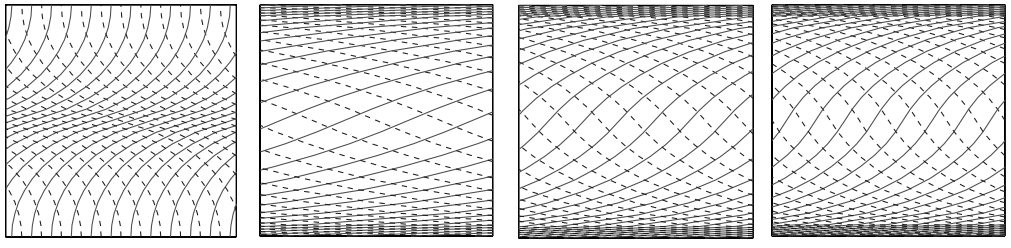


**Fig. 7 Optimal fiber paths for maximum compressive failure load (CC-CC laminate with four-designed layers, $\theta = \theta(y)$).**

**Table 6 Comparison between VS and optimal constant-stiffness laminates; four-designed layers, $\theta = \theta(y)$**

| Boundary conditions | Laminate | Compressive failure load, $\lambda_2^f$ | Load carrying capacity improvement, % | Normalized buckling load | Buckling load improvement, % |
|---|---|---|---|---|---|
| SS-CC | $[\pm 45/90/0/0/0/90]_s$ | 5.14 | —— | 1.0 (14000 lb) | —— |
| —— | $[\pm\langle 5\vert 0\rangle/\pm\langle 0\vert 10\rangle/\pm\langle 90\vert 0\rangle/\pm\langle 84\vert 86\rangle]_s$ | 6.08 | 18.3 | 1.52 | 52.0 |
| CC-CC | $[\pm 45/0/90/90/0/90/0]_s$ | 4.52 | —— | 1.0 (20057 lb) | —— |
| —— | $[\pm\langle 15\vert 90\rangle/\pm\langle 24\vert 0\rangle/\pm\langle 50\vert 0\rangle/\pm\langle 60\vert 0\rangle]_s$ | 5.92 | 31.0 | 1.75 | 75.0 |

**Table 7 Comparison between VS and quasi-isotropic laminates; two-designed layers, $\theta = \theta(x)$**

| Boundary conditions | Laminate | Normalized buckling load | Buckling load improvement, % | Failure load, $\lambda_2^f$ | Failure load improvement, % |
|---|---|---|---|---|---|
| SS-CC | $[\pm 45/0/90]_{2s}$ | 1.0 | 71.0 | 4.02 | 6.0 |
| —— | $[\pm\langle 26\vert 18\rangle/\pm\langle 75\vert 0\rangle]_{2s}$ | 1.71 | —— | 4.26 | —— |
| CC-CC | $[\pm 45/0/90]_{2s}$ | 1.0 | 47.0 | 3.54 | 28.8 |
| —— | $[\pm\langle 26\vert 0\rangle/\pm\langle 90\vert 5\rangle]_{2s}$ | 1.47 | —— | 4.56 | —— |

**Table 8 Comparison between VS and quasi-isotropic laminates; four-designed layers**

| Boundary conditions | Angle variation | Laminate | Normalized buckling load | Buckling load improvement, % | Compressive failure load, $\lambda_2^f$ | Failure load improvement, % |
|---|---|---|---|---|---|---|
| SS-CC | —— | $[\pm 45/0/90]_{2s}$ | 1.0 | —— | 4.02 | —— |
| —— | $\theta = \theta(x)$ | $[\pm\langle 0\vert 50\rangle/\pm\langle 53\vert 45\rangle/\pm\langle 0\vert 55\rangle/\pm\langle 85\vert 43\rangle]_s$ | 1.8 | 80.0 | 3.78 | −6.0 |
| —— | $\theta = \theta(y)$ | $[\pm\langle 65\vert 36\rangle/\pm\langle 85\vert 10\rangle/\pm\langle 90\vert 5\rangle/\pm\langle 90\vert 5\rangle]_s$ | 2.18 | 118.0 | 0.54 | −86.6 |
| CC-CC | —— | $[\pm 45/0/90]_{2s}$ | 1.0 | —— | 3.54 | —— |
| —— | $\theta = \theta(x)$ | $[\pm\langle 16\vert 30\rangle/\pm\langle 80\vert 22\rangle/\pm\langle 25\vert 34\rangle/\pm\langle 85\vert 29\rangle]_s$ | 1.5 | 50.0 | 4.52 | 27.7 |
| —— | $\theta = \theta(y)$ | $[\pm\langle 45\vert 51\rangle/\pm\langle 70\vert 0\rangle/\pm\langle 73\vert 5\rangle/\pm\langle 75\vert 5\rangle]_s$ | 2.61 | 161.0 | 2.28 | −35.6 |

Varying the stiffness in the $y$ direction (perpendicular to the applied load) produces more improvements than that of the $x$ direction. On the other hand, a close look at Tables 7 and 8 reveals that the variable-stiffness laminates with $\theta = \theta(x)$ optimized for maximum buckling loads have, in general, better strength performance than their quasi-isotropic counterparts, especially for the CC-CC panels. Slight degradation in the strength performance of the SS-CC panel with respect to its quasi-isotropic baseline is encountered. In contrast, laminates with $\theta = \theta(y)$ optimized for maximum buckling loads fail dramatically at load levels much lower than those for quasi-isotropic ones.

It is observed that designs obtained for maximum compressive failure loads have straight fiber layers, while designs obtained for maximum buckling loads do not. It is intuitive that the steered fibers are more efficient than the straight fibers in transferring the loads from regions to the others over the structure. As previously demonstrated, this is a key mechanism that the steered fibers use to improve the buckling performance. Also, the nonuniform prebuckling in-plane stress distribution generated by the steered fibers has significant effect on the buckling load. To demonstrate these mechanisms, two laminates with different fiber orientation variations, with four-designed plies, are considered. These laminates are the SS-CC laminate with $\theta = \theta(x)$ and the CC-CC laminate with $\theta = \theta(y)$. First we consider the prebuckling stress resultant distributions of the SS-CC laminate. For the constant-stiffness quasi-isotropic laminate, the axial stress resultant $N_x$ is compressive and constant, and $N_y$, $N_{xy}$ are zero over the entire panel. For the variable-stiffness laminate, on the other hand, $N_x$ is compressive and constant over the entire panel, but $N_y$ is a function of location along the $x$ direction as shown in Fig. 9. It is clear that the center section of the panel experiences tension, whereas the loaded edges ($x = 0$, $x = a$) have transverse compression. Such an in-plane stress distribution is certainly responsible for improving the buckling performance since the tensile stresses induced at the panel center section, where the panel is prone to buckling, have a stabilizing effect. Second, we consider the CC-CC laminate with $\theta = \theta(y)$. For the CC-CC quasi-isotropic panel, the stress resultant distributions are similar to those for the previous SS-CC quasi-isotropic one. For the variable-stiffness panel, the stiffness variation along the $y$ coordinate has important influence on the stress resultant distribution along the $x$ coordinate $N_x$

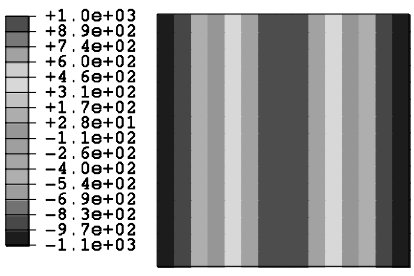


**Fig. 9 Prebuckling stress resultant, $N_y$ (SS-CC laminate with four-designed plies, $\theta = \theta(x)$).**

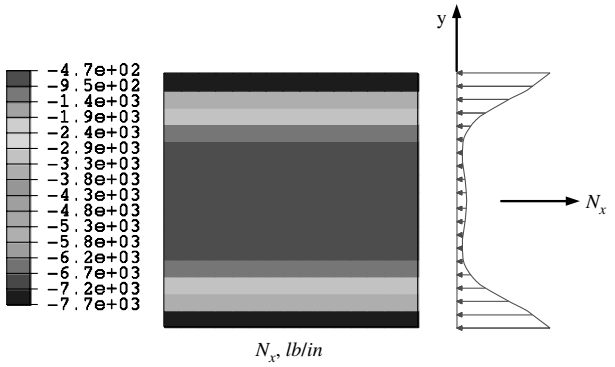


**Fig. 10 Prebuckling stress resultant, $N_x$ (CC-CC laminate with four-designed plies, $\theta = \theta(y)$).**

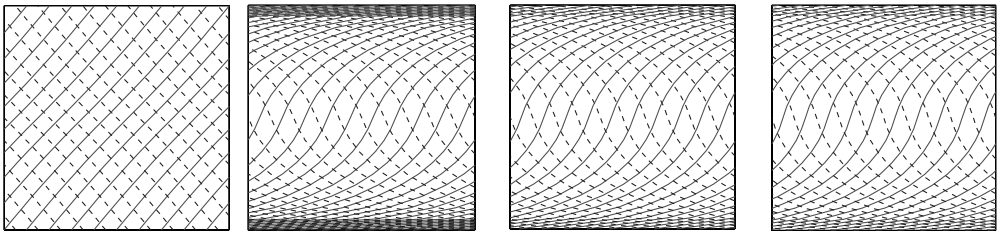


**Fig. 11 Optimal fiber paths for maximum buckling load (CC-CC laminate with four-designed layers, $\theta = \theta(y)$).**

as shown in Fig. 10. This distribution is similar to the one shown in Fig. 8 in that the total applied load along the $x$ direction is distributed in the panel such that a larger portion of the loads are near the transverse edges of the panel, with the center section of the panel carrying a smaller portion of the applied load. However, as shown in Fig. 10, herein the majority of the applied load has been transferred toward the panel edges, where out-of-plane deflections are suppressed. This, actually, results from the fact that the local axial stiffness is high at the transverse edges where the fiber orientation, in most of the laminate layers, is almost zero (see Fig. 11), and the fiber orientation in the panel center is relatively high. As a consequence, the center section of the panel is left without carrying significant load, hence is much less prone to buckling.

As far as manufacturability is concerned, it can be noticed that the laminates designed for maximum buckling loads have fiber paths with large curvatures, whereas the fiber paths for the laminates designed for maximum failure loads, especially for panels with $\theta = \theta(x)$, are smoother, and hence possibly easier to manufacture. Accordingly, it can be concluded that designing laminates for maximum strength is the choice that may be adopted to satisfy the structural and technological requirements.

## VIII. Conclusions

In this paper, design tailoring for the pressure pillowing problem of a fuselage panel bounded by two frames and two stringers was addressed using tow-placed steered fibers. The panel was modeled as a two-dimensional plate and loaded by out-of-plane pressure and in-plane loads. Using the ABAQUS scripting interface, a Python script was developed to perform the linear and geometrically nonlinear finite element analyses of variable stiffness panels. The design objective was to determine the optimal fiber paths within each ply of the laminate lay-up for maximum strength and buckling performance. A global SA optimizer was used to solve the optimization problems. Optimal designs were obtained for different loading cases and boundary conditions. As a basis of comparison, a practical constant-stiffness quasi-isotropic design was used. It was shown that by tailoring the fiber paths within each ply of the laminate lay-up, the load carrying capacity and the buckling load of the structure can be substantially improved compared with the traditional quasi-isotropic design with straight fibers. It was also shown that laminates optimized for maximum failure loads have buckling loads that are also significantly higher than those for quasi-isotropic laminates. On the other hand, the substantially improved buckling performance obtained for laminates optimized for maximum buckling loads may come at the expense of degraded strength performance. It was concluded that designing laminates for maximum strength may be a better choice to satisfy the structural and manufacturing requirements. If buckling loads are to be maximized it is necessary to impose strength constraints during the optimization process.

Finally, it should be mentioned that the load cases used in the present paper have been selected to demonstrate the variable-stiffness concept and the approach of addressing particular problems in aircraft structure. Other load cases such as pressure and fuselage torsion are important load combinations that are likely to produce different interesting cases.

## References

[1] Biggers, S. B., and Srinivasan, S., "Compression Buckling Response of Tailored Rectangular Composite Plates," *AIAA Journal*, Vol. 31, No. 3, 1993, pp. 590–596. doi:10.2514/3.61543

[2] Biggers, S. B., and Pageau, S. S., "Shear Buckling Response of Tailored Rectangular Composite Plates," *AIAA Journal*, Vol. 32, No. 5, 1994, pp. 1100–1103. doi:10.2514/3.12107

[3] Hyer, M. W., and Charette, R. F., "The Use of Curvilinear Fiber Format in Composite Structure Design," *Proceedings of the AIAA/ASME/ASCE/AHS/ASC 30rd Structures, Structural Dynamics and Materials Conference*, AIAA, New York, 1989.

[4] Nagendra, S., Kodiyalam, S., Davis, J. E., and Parthasarathy, V. N., "Optimization of Tow Fiber Paths for Composite Design," *Proceedings of the AIAA/ASME/ASCE/AHS/ASC 36rd Structures, Structural Dynamics and Materials Conference*, AIAA, New York, April 1995, pp. 1031–1041; also AIAA Paper 95-1275.

[5] Gürdal, Z., and Olmedo, R. A., "In-Plane Response of Laminates with Spatially Varying Fiber Orientations: Variable Stiffness Concept," *AIAA Journal*, Vol. 31, No. 4, 1993, pp. 751–758. doi:10.2514/3.11613

[6] Olmedo, R. A., and Gürdal, Z., "Buckling Response of Laminates with Spatially Varying Fiber Orientations," *Proceedings of the AIAA/ASME/ASCE/AHS/ASC 34rd Structures, Structural Dynamics and Materials Conference*, AIAA, New York, April 1993, pp. 2261–2269;also AIAA Paper 93-1567.

[7] Waldhart, C., Gürdal, Z., and Ribbens, C., "Analysis of Tow Placed, Parallel Fiber, Variable Stiffness Laminates," *Proceedings of the AIAA/ASME/ASCE/AHS/ASC 37rd Structures, Structural Dynamics and Materials Conference*, AIAA, New York, April 1996, pp. 2210–2220; also AIAA Paper 96-1569.

[8] Parnas, L., Oral, S., and Ceyhan, U., "Optimum Design of Composite Structures with Curved Fibers," *Composites Science and Technology*, Vol. 63, 2003, pp. 1071–1082. doi:10.1016/S0266-3538(02)00312-3

[9] Boitnott, R. L., Starnes, J. H., Jr., and Johnson, E. R., "Nonlinear Response and Failure of Pressurized Composite Curved Panels," *Journal of Aerospace Engineering*, Vol. 8, No. 3, July 1995, pp. 129–138. doi:10.1061/(ASCE)0893-1321(1995)8:3(129)

[10] Alhajahmad, A., Abdalla, M. M., and Gürdal, Z., "Design Tailoring for Pressure Pillowing Using Tow-Placed Steered Fibers," *38th International SAMPE Technical Conference*, Society for the Advancement of Material and Processing Engineering, Covina, CA, Nov. 2006.

[11] Alhajahmad, A., Abdalla, M. M., and Gürdal, Z., "Design Tailoring for Pressure Pillowing Using Tow-Placed Steered Fibers," *Journal of Aircraft*, Vol. 45, No. 2, 2008, pp. 630–640. doi:10.2514/1.32676

[12] ABAQUS Version 6.7 Documentation. ABAQUS, Inc., 2007.

[13] Goffe, W. L., Ferrier, G. D., and Rogers, J., "Global Optimization of Statistical Functions with Simulated Annealing," *Journal of Econometrics*, Vol. 60, Nos. 1–2, Jan.–Feb. 1994, pp. 65–99. doi:10.1016/0304-4076(94)90038-8

[14] Jones, R. M., *Mechanics of Composite Materials*, 2nd ed., Taylor and Francis, Philadelphia, 1998, Chap. 2.

[15] Hyer, M. W., and Lee, H. H., "The Use of Curvilinear Fiber Format to Improve Buckling Resistance of Composite Plates with Central Circular Holes," *Composite Structures*, Vol. 18, No. 3, 1991, pp. 239–261. doi:10.1016/0263-8223(91)90035-W

[16] Gürdal, Z., Haftka, R. T., and Hajela, P., *Design and Optimization of Laminated Composite Materials*, Wiley, New York, 1998.